Review

A Review of Acoustic Metamaterials and Phononic Crystals

Junyi Liu [1], Hanbei Guo [2] and Ting Wang [3,4,5],*

[1] College of Engineering, Huazhong Agricultural University, Wuhan 430070, China; LIUJUNYI@webmail.hzau.edu.cn

[2] Wuhan Second Ship Design and Research Institute, Wuhan 430064, China; ghb901127@foxmail.com

[3] School of Naval Architecture & Ocean Engineering, Huazhong University of Science and Technology, Wuhan 430074, China

[4] Collaborative Innovation Center for Advanced Ship and Deep-Sea Exploration (CISSE), Shanghai 200240, China

[5] Hubei Key Laboratory of Naval Architecture and Ocean Engineering Hydrodynamic (HUST), Wuhan 430074, China

* Correspondence: wang_ting@hust.edu.com

check for updates

Abstract: As a new kind of artificial material developed in recent decades, metamaterials exhibit novel performance and the promising application potentials in the field of practical engineering compared with the natural materials. Acoustic metamaterials and phononic crystals have some extraordinary physical properties, effective negative parameters, band gaps, negative refraction, etc., extending the acoustic properties of existing materials. The special physical properties have attracted the attention of researchers, and great progress has been made in engineering applications. This article summarizes the research on acoustic metamaterials and phononic crystals in recent decades, briefly introduces some representative studies, including equivalent acoustic parameters and extraordinary characteristics of metamaterials, explains acoustic metamaterial design methods, and summarizes the technical bottlenecks and application prospects.

Keywords: acoustic metamaterial; phononic crystal; effective negative parameters; band gaps; research overview

1. Research Background

Noise is one of the four major public hazards in the world which seriously affect people's daily life and work. Noise is caused by the random vibration of objects, mainly mechanical vibrations. Mechanical vibration itself is also harmful to mechanical structures and engineering equipment, and even more serious for precision machine tools and instruments. Mechanical vibrations not only cause fatigue and wear of mechanical equipment and affects its performance, but also greatly shorten the service life of the equipment. At the same time, noise generated by mechanical equipment will reduce people's quality of life, threatening their well-being. The most direct harm to the human body caused by noise is damage to hearing, and damage to the central nervous system of a person. Low frequency vibrations and noise are able to travel further, so if captured by the enemy sonar, they can expose and endanger underwater vehicles. Therefore, in order to improve people's living environment and survival capability, it is necessary to develop vibration suppression and noise reduction techniques [1].

There are three main ways to control vibration and noise [2]. The first is to control the source, design and manufacture products with small noise, low vibration or silent; the second is to control the propagation path, mainly via isolation, absorption and attenuation, etc.; the third is to protect the receiver. As people's requirements for product functions become higher and higher, product structures

become more and more complex, and it has become increasingly difficult to reduce noise from the source. Moreover, the receivers are often changing their locations, so techniques to protect the receiver are not reasonable. Therefore, it is a more sensible choice to try to reduce vibration and noise in the propagation path. The ways to control noise are divided into active controls and passive controls. Here we mainly discuss passive control methods. In passive control, various vibration suppression and sound insulation materials have been developed rapidly in recent years, and people have also designed various vibration isolators and sound absorbers. There are some limitations in traditional vibration reduction techniques [3], such as vibration insulation, dynamic vibration absorption and damping vibration absorption. The equipment must be larger for vibration insulation technology. What's more, it shows a narrow frequency band and is greatly affected by the environment. For dynamic vibration absorption, the disadvantages are that it focuses on a large mass and has a narrow frequency band too. However, the damping vibration absorption only has an impact on the intermediate and the high frequencies. In the low frequencies, the effect is poor. Traditional sound insulation materials generally use rigid plates, in order to isolate low-frequency sound waves of hundreds of Hertz [4]. A concrete partition with a thickness of 1 m needs to be designed. Traditional sound-absorbing materials are mostly porous structures, such as organic fiber materials, rock wool, mineral wool, etc. These materials mainly rely on small holes from the surface to the inside to attenuate sound waves [5]. According to the frequency range, sound waves can be divided into the following types: low frequency, intermediate frequency and high frequency. Noise in the low-frequency range has strong penetrating power and dissipates slowly during propagation, making it difficult to control the sound waves; low-frequency sound waves can also resonate with certain important organs of the human body, affecting health. Therefore, it is necessary to strengthen the research on low frequency noise and vibration control. No matter whether the above-mentioned vibration-isolating materials or sound-absorbing materials are considered, they basically absorb medium and high frequency sound waves, and the effect on isolating low-frequency noise is not significant. In recent decades, research on artificial composite materials has become the focus of many scholars, and acoustic metamaterials and phononic crystals have been discussed in this context.

2. Basic Concept of Acoustic Metamaterials and Phononic Crystals

2.1. Proposals for Acoustic Metamaterials and Phononic Crystals

"Metamaterials" refer to a class of materials that are artificially synthesized and have properties different from those of conventional materials without violating objective physical laws. The concept of metamaterials first came from electromagnetics. In 1968, Veselago [6], a theoretical physicist in the former Soviet Union, discovered that the dielectric properties and the permeability of electromagnetic materials are both negative, which is different from conventional materials with positive material parameters, and thus theoretically proposed electromagnetic metamaterials. This kind of optical material with negative dielectric constant and magnetic permeability has a negative refractive index. The incident and outgoing streams are on the same side of the normal line instead of the opposite side. The wave vector K, the electric field intensity E, and the magnetic field intensity H constitute a left-handed relationship. This material is called a left-handed material, also known as a double negative material. An analog optical metamaterial is designed using a structure much smaller than the sub-wavelength size to obtain an acoustic metamaterial [7]. The effective parameters of the acoustic metamaterial become negative within specific frequency ranges, called band gaps (see Figures 1 and 2). For natural materials, the material parameters such as the mass density, Young's modulus, Poisson's ratio, are positive in natural circumstances, while with artificial construction, the effective material parameters may turn negative within specific frequency ranges. When mechanical waves propagate in this type of structure, due to the modulation of the structure, the propagation of mechanical waves is hindered, thereby achieving a sound absorption and vibration isolation effect [8].
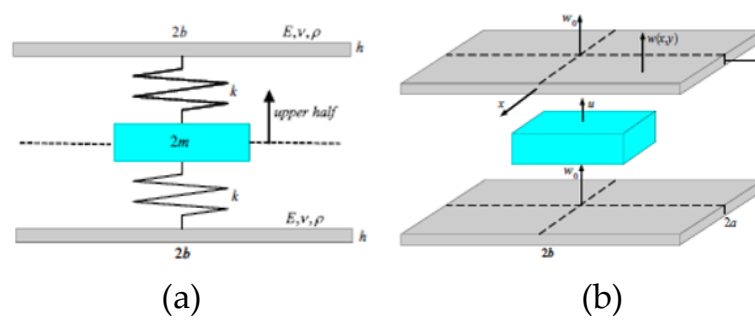
Figure 1. A unit cell of a typical acoustic metamaterial plate: (**a**) front view; (**b**) perspective view [7].
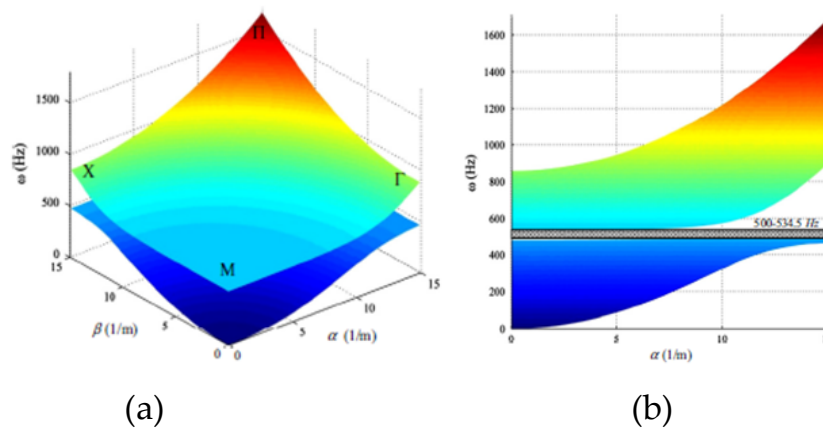
Figure 2. Dispersion surfaces and band gap of the above metamaterial: (**a**) dispersion surfaces; (**b**) stopband (gray rectangle) [7].

In the 1990s, the concept of a phononic crystal was modeled after the concept of a photonic crystal. By artificially designing the structure and defects of the photonic crystal, the propagation of light waves can be controlled [9–11]. Later, it was discovered that elastic waves propagate in a periodic elastic composite medium, which also produces a similar band gap phenomenon (see Figure 3) [12]. In 1992, Sigalas et al. [13] buried spherical objects in a matrix material in a periodic lattice structure arrangement. Under the action of external sound waves, the composite produced an acoustic band gap phenomenon, and thus phononic crystals were theoretically synthesized for the first time. Kushwaha et al. [14] formally proposed the concept of phononic crystals in 1993, that is, a material with a periodic elastic medium structure with a phononic forbidden band. Similarly, by changing the internal structure and defects of the phononic crystal, the propagation path of the elastic wave can be artificially adjusted, thereby achieving the purpose of vibration isolation and noise reduction [15].
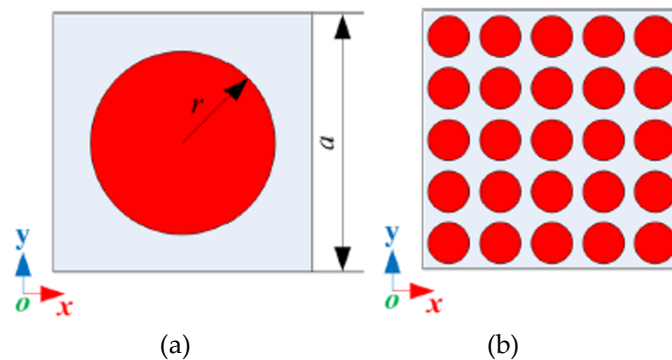
Figure 3. Proposed metamaterial with defect states [12].

The biggest difference between a phononic crystal and an acoustic metamaterial is that its resolution is limited by anisotropy and the lattice constant, but the acoustic metamaterial is basically unrestricted [16]. Phononic crystals require the lattice size to be the same order of magnitude as the wavelength in the direction of sound wave propagation, while the acoustic metamaterial is able to restrain the waves with much larger wavelength than the lattice size. The acoustic metamaterial is composed of many tiny units with mechanical resonators, and each unit can avoid interference with each other. There are basically no restrictions on the structure size of the resonator. Moreover, the mechanisms of the phononic crystals and acoustic metamaterials are different. Elastic waves in phononic crystals may be reflected and scattered at the interfaces of the inner and outer materials and the propagation waves, reflected waves, and scattered waves interfere, which leads to band gaps. The acoustic metamaterials absorb the elastic wave energy into the local resonators to block the waves. Therefore, the practical application range of the acoustic metamaterial is wider.

2.2. Band Structure Calculation Method of Phononic Crystal and Acoustic Metamaterials

The research on forbidden bands in phononic crystals and acoustic metamaterials mainly focuses on the calculation of elastic wave forbidden bands. At present, there are several mature methods for calculating forbidden bands, such as the transfer matrix method, the plane wave expansion method, the finite difference time domain method and the multiple scattering method, etc.

The transfer matrix method [17,18] is a method of converting the wave equation into the form of a transfer matrix equation and solving the eigenvalues. This method starts with the basic equations including state parameters (stress, particle velocity, etc.) to obtain the transfer equation of a flat solid medium, then obtains the boundary conditions according to the characteristics of the surrounding medium and the intermediate medium, and finally obtains the solution of the system. This method is mainly used for the calculation of band gaps of phononic crystal and acoustic metamaterial in a one-dimensional model. Because the transfer matrix is generally small and is an analytical solution, its calculation effort is small.

The plane wave expansion method [14,19–22] is the earliest and most widely used method in the theoretical analysis of phononic crystals and acoustic metamaterials. In this method, the physical quantities such as displacements and elastic constants in the wave equation are expanded by a Fourier transform in the form of superposition of plane waves in the inverse lattice space, and then the wave equation is solved to obtain the dispersion relationship between the characteristic frequency and the wave vector, that is, the band structure. The plane wave expansion method can be used for two-dimensional and three-dimensional band structures. In the calculation of solid [14,19,20], liquid-liquid [21,23,24], and solid-gas [25–28] systems, great success was achieved with the band gaps of phononic crystals and acoustic metamaterials. However, this method has certain limitations, as its convergence is slow, and it may even diverge during expansion, which makes it impossible to solve.

The finite-difference time-domain method [29,30] discretizes partial differential equations by discretizing time and space, transforms the partial differential equations into differential equations, and then uses numerical calculation methods to solve all vibrations at three points during wave propagation. Parameters are a function of time. This method can simulate a variety of complex periodic structures, and can accurately simulate the non-uniformity, anisotropy, nonlinear problems and dispersion characteristics of the medium. At the same time, the method can calculate the characteristics of the band structure in the periodic structure and the transmission and reflection in the finite structure. When using this method to calculate the instantaneous nonlinear response of a phononic crystal or an acoustic metamaterial, attention should be paid to the numerical stability and convergence.

Because the plane wave expansion method cannot solve the problem of solid scatterers in a liquid matrix, scholars have proposed a multiple scattering method based on the Korringa-Kohn-Rostoker (KKR) theory in the calculation of the electronic band structure [31]. The theory of multiple scattering of elastic waves holds that the frequency band structure of a crystal depends on the Mie scattering between spheres. By calculating the scattering of sound waves from other spheres incident on the

surface of a single sphere, the characteristic frequency equation can be solved [32]. This method is very suitable for the calculation of phononic crystals with special structures. For this kind of band structure, general plane waves cannot give accurate solutions. The multiple scattering method also has disadvantages. It is complicated to calculate and difficult to use.

In addition to the above methods, there are some other methods to calculate the band structures of phononic crystals and acoustic metamaterials, such as the finite element method and the spectral element method. Every method has its own limitations. When analyzing different structural forms of phononic crystal and acoustic metamaterials, we should consider its structural form, the structural complexity, the structural dimensions and others to choose the exact one. At the same time, based on the existing methods, we should also develop new ones with fast calculation and good convergence to lay the foundation for the follow-up research.

3. Equivalent Acoustic Parameters of Acoustic Metamaterials

Mass density ρ and bulk elastic modulus K are two key parameters of acoustic materials. They determine the propagation characteristics of acoustic waves in the medium. Both the sound velocity and the characteristic impedance of a medium are expressed by these two parameters: the speed of sound $c = \sqrt{K/\rho}$ and the characteristic impedance of the medium $Z = \sqrt{K\rho}$. In conventional materials, both the mass density ρ and the bulk elastic modulus K are positive and depend on the material composition and microstructure of the media. However, if local resonance units are introduced into the material to enhance the acoustic-matter interaction, it is possible that the equivalent acoustic parameters can become negative within a specific frequency range not found in natural materials. Based on the resonance mechanism, we can achieve negative equivalent mass density and equivalent bulk modulus, as well as extraordinary acoustic parameters such as negative refractive index [33].

4. Typical Types of Acoustic Metamaterials and Phononic Crystals

In 2000, Liu et al. [32] used the "core-shell structure" for the first time to make an acoustic metamaterial. Based on the "core-shell structure" concept scholars have further developed the following other structures.

4.1. Structures Composed of Functional Units with Certain Mechanical Characteristics

The spring-mass model is periodically arranged on a two-dimensional thin plate, which is a common local resonance model. This model has a simple structure, and the resonance of the vibrator is also easy to adjust. It is frequently used in real life. There are three main components of this structure. Component 1 is a mass of mass m, component 2 is a matrix of mass M, and component 3 is a spring connecting components 1 and 2.

In 2011, Huang et al. [34] proposed two types of mass spring structures with local resonators and performed equivalent simulations, and found that they have negative effective elastic modulus and selective filtering. In 2016, Zhu et al. [35] periodically arranged a spring-vibrator resonance unit on a stiffened plate to obtain a local resonance stiffened plate structure (see Figure 4) and simulated its performance. They found that the structure can generate a lower frequency local resonance band gap and widen the high frequency Bragg band gap compared to ordinary stiffened plates.
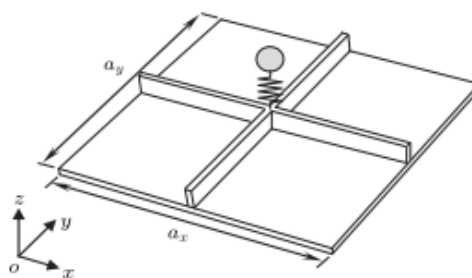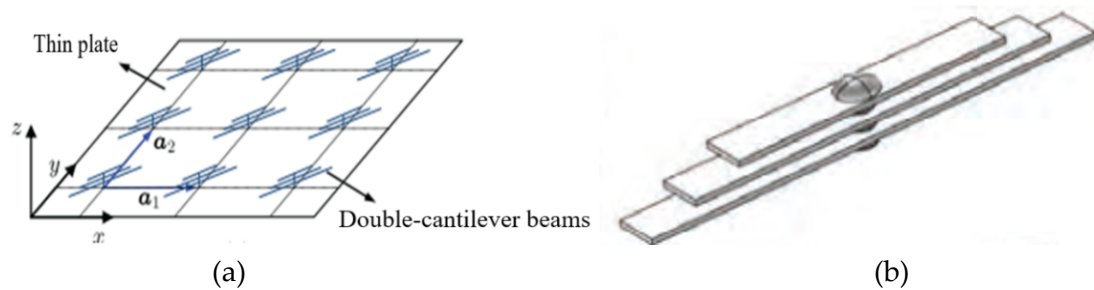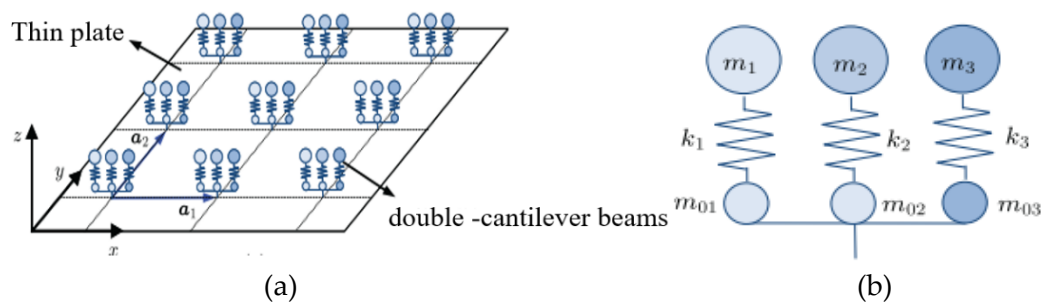

Figure 4. Schematic diagram of the unit cells of a locally resonant stiffened plate [35].

The same year, Wu et al. [36] obtained a multi-frequency local resonance type phononic crystal plate by periodically attaching multiple double cantilever structures on a thin plate (see Figures 5 and 6). Through their theoretical research, it is found that the structure can generate multiple low-frequency bending wave forbidden bands, and the bending vibration of the plate is significantly reduced in the band gap range.


(a)   (b)

Figure 5. Schematic diagram of a multi-frequency locally resonant phononic plate: (**a**) Schematic diagram of the phononic plate with several periodic unit cells; (**b**) schematic diagram of the attached double -cantilever beams [36].

(a)   (b)

Figure 6. Simplified model of the proposed multi-frequency locally resonant phononic plate: (**a**) Schematic diagram of the simplified model with several periodic unit cells; (**b**) The low-frequency equivalent "mass-spring-mass" system of the attached double-cantilever beams [36].

In 2019, Ma et al. [37] proposed a damping structure with multi-band gap characteristics based on the spring-vibrator resonance unit (see Figure 7), and found that the structure has the characteristics of low frequency band and low frequency limit.
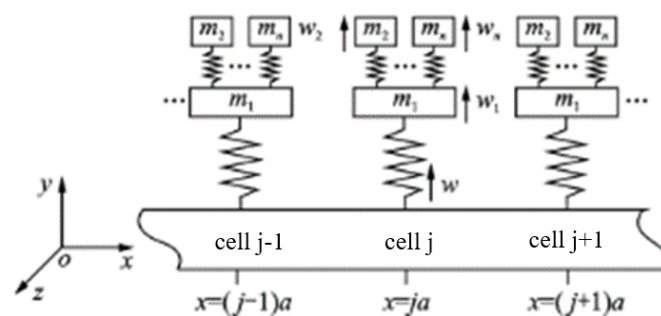
**Figure 7.** Schematic diagram of the suppressors periodically arranged on the base beam [37].

At present, referring to the idea "local resonance phononic crystals", a kind of local artificial periodic structure can be constructed by periodically attaching spring-mass units to traditional engineering structures such as rods, beams and plates. The structures described above do not need to destroy the uniformity and integrity of the substrate structure, which has wide applicability in practical

engineering. Afterwards, the research will focus on the constitution of more local resonance common engineering structures, and study their bandgap characteristics and vibration reduction characteristics, to provide more ideas for the vibration reduction design of common engineering structures.

*4.2. Helmholtz Resonator Periodic Arrangement Structures*

Helmholtz resonance refers to the resonance phenomenon of air in a cavity. A container made using this phenomenon is called a Helmholtz resonance cavity. It comprises a rigid container with a known volume and a shape close to a sphere. The container has a narrow opening at one end and a small opening at the other end. Helmholtz resonators can filter sounds of specific frequencies.

In 2006, Fang et al. [38] firstly proposed an acoustic metamaterial composed of a periodic one-dimensional Helmholtz resonator cavity with acoustic inductance and capacitance (see Figure 8). Experiments have proved that this material can achieve negative elastic modulus. They research found that when the frequency of the acoustic wave is close to the resonance frequency, the frequency at the exit of the resonant cavity will be opposite to the frequency of the external acoustic wave, thereby achieving a transmission band gap.

(a) (b)
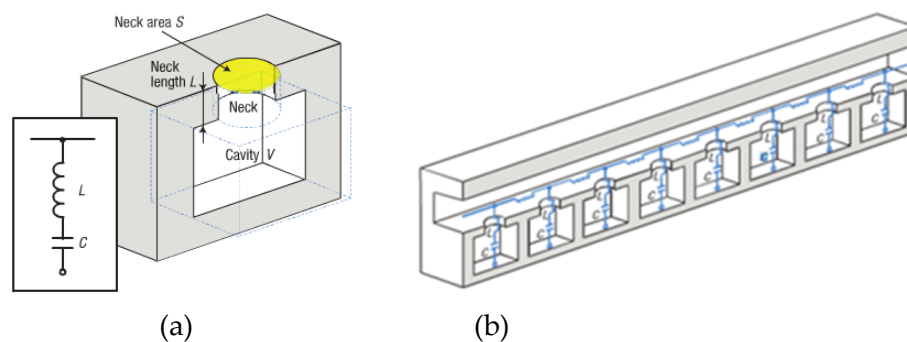
Figure 8. The schematic diagram of proposed structures: (**a**) One-dimensional Helmholtz resonator; (**b**) Helmholtz resonator composed of periodic arrangements [38].

In 2017, Jiang et al. [39] adopted a double-opening internal and external cavity design to obtain a double-opening Helmholtz periodic structure (see Figure 9). It is found that the structure has good low-band gap characteristics, and its lowest band-gap section is 86.9–138.2 Hz. At a certain outer diameter, the low-band gap is affected by the arc length of the cavity, the internal and external cavity spacing, and the spacing between cells.


(a) (b)
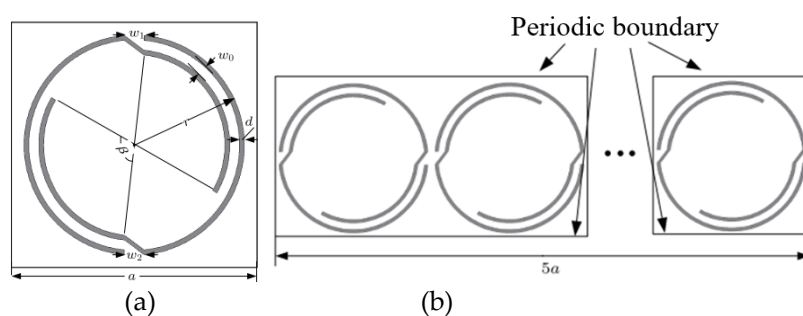
Figure 9. The schematic diagram of the double-opening Helmholtz periodic structure: (**a**) The unit structure's cross section of the double-split Helmholtz resonant structure; (**b**) The finite structure with 5 cells of the double-split Helmholtz resonant structure [39].

In 2018, Yu et al. [40] changed the rigidity of Helmholtz resonators (HRs) and designed a tube with a periodically arranged elastic HR (see Figure 10). Their research found that for a single Helmholtz cavity unit of the same size, the resonant frequency of the elastic HR is much lower than that of the

rigid HR. Secondly, the factor determining the elastic HR resonance frequency is the top plate, not the cavity size. For periodic pipelines, periodic elastic HR is more conducive to generating low-frequency and wide-band gaps.

Helmholtz resonators take advantage of the resonance characteristics of air, and they have good advantages in light weight and low frequency design only by structural design without additional mass, which has been a great basic model to create acoustic metamaterials recognized by many scholars. Up to now, metamaterials made from Helmholtz resonators have been widely used in the engineering field, like for pipe sound absorption. Nevertheless, in the periodic structure design of Helmholtz resonators, the local resonance region is small due to the number and the depth of openings, which results in the need for a large volume to obtain low-frequency characteristics.

(a) (b)
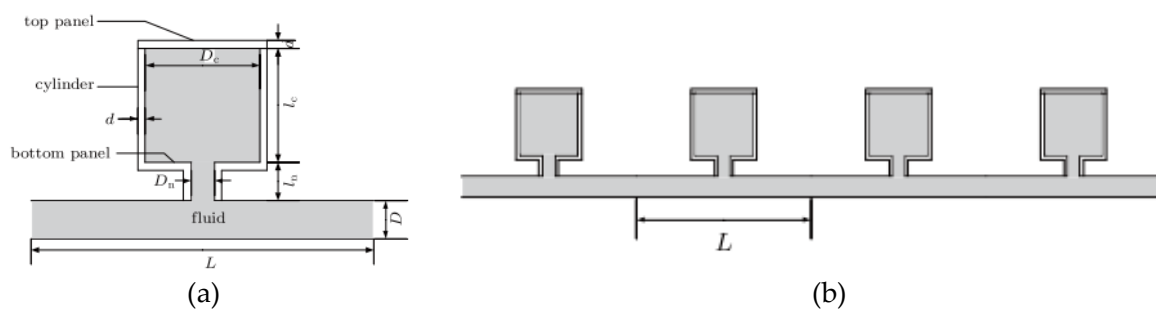
Figure 10. Schematic diagram of the proposed structure: (**a**) Sketch of an elastic HR; (**b**) Sketch of an infinite periodic pipe with elastic HRs [40].

4.3. Thin Film Acoustic Metamaterials

The film-type acoustic metamaterial unit is a film that is tensioned and fixed on the peritoneal ring, and then a rigid mass unit is fixed on the circular film [41,42]. The working mechanism of the thin film acoustic metamaterial is to increase the energy density of low-frequency sound waves inside the metamaterial by increasing the resonance mode. When the metal sheet is beaten, the contact boundary with the thin film contains enhanced elastic curvature energy, and the coupling effect with the acoustic wave is cancelled to achieve Resonant cavity-like sound absorption purposes [43].

In 1991, Hashimoto et al. [44] first proposed a membrane structure with additional masses, the so-called membrane with additional weights (MAW), and found that this structure can improve sound insulation in the low frequency range through sound insulation experiments under normal incidence effects. In 2008, Yang and Mei of The Hong Kong University of Science and Technology formally proposed the concept of "thin film acoustic metamaterial", and pointed out that it is composed of an elastic film, an additional mass, and a supporting structure of a fixed film. The structure was found to have an acoustic band gap in the frequency range of 200–300 Hz [45]. Later, it was found that the structure composed of four layers of thin film materials with different sound insulation frequency bands and different mass masses can achieve 50–1000 Hz wide-band sound insulation, and its sound insulation is as high as 40 dB [46]

In 2019, He et al. [47] designed a new type of thin film acoustic metamaterial by embedding a piezoelectric mass connected to an external circuit into a tensioned elastic membrane and fixed on a metal frame (see Figure 11). They found that the structure has good sound insulation performance in the 20–1200 Hz frequency band and there are two sound insulation peaks above 50 dB and one adjustable sound insulation peak. Secondly, by adjusting the circuit parameters, the tunability of the sound insulation performance of the material can be achieved.
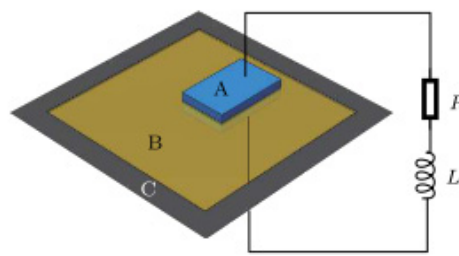
Figure 11. The structural sketch [47].

The lateral local resonance metamaterial structure proposed by Wang et al. [48,49] can also suppress low frequency noise (see Figure 12). By analyzing the energy band structure diagram of the metamaterial, they found that the metamaterial plate could generate two low-frequency band gaps by the equivalent mass. The vibration power flow of metamaterial plate was obtained by using the finite element method and the energy flow method, so as to reveal its vibration suppression mechanism.
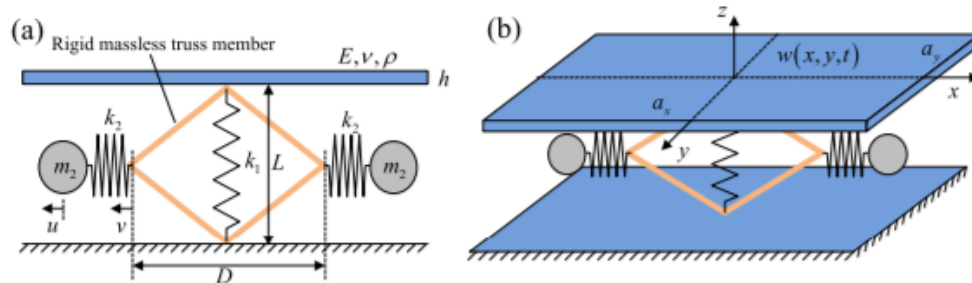

Figure 12. The unit cell of the metamaterial plate: (**a**) front view, (**b**) perspective view [48].

In 2020, Zhou et al. [50] proposed a polymorphic anti-resonance cooperative thin-film acoustic metamaterial (see Figure 13). The material consists of four metal foils and a cross-shaped flexible ethylene-vinyl acetate (EVA) material swing arm attached to the surface of a polyimide (PI) film, and uses EVA material as a frame. The study found that the material has achieved widening of the low frequency sound insulation band and improvement of sound insulation.
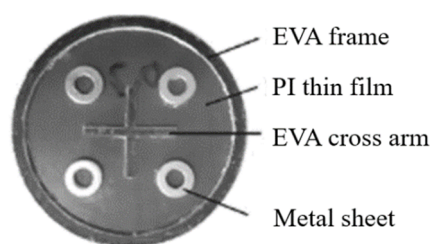

Figure 13. A small size MAM experimental sample [50].

The advantage of this type of acoustic metamaterials is that the band gap frequency domain is very low, which means that they can suppress low-frequency elastic wave propagation. However, the structure is too thin with low stiffness to bear weight, which limits its application in practical engineering.

4.4. Space Coiling Structures

Research on local resonance acoustic metamaterials has made great progress, but it has disadvantages such as narrow frequency band and difficult design and manufacture. In response to the abovementioned shortcomings, scholars have introduced the coiled space type structure into acoustic metamaterials, and designed coiled space type acoustic metamaterials. The sound absorption mechanism of the curly

space structure is to allow sound waves to propagate in the coiled space, increasing the propagation time and reducing the effective phase velocity [51,52].

In 2015, Li et al. [53] designed a curly space structure composed of a Jerusalem cross groove air matrix periodically arranged in a square lattice. It is found that the structure can generate a large band gap in low frequency mode, and the band gap formation mechanism is the resonance mode of the internal cavity of the cross groove structure.

The same year, Wang et al. [54] designed an S-shaped groove structure in a square lattice (see Figure 14). They found that the structure can produce a more complete and larger band gap in the lower frequency range compared to a Jerusalem cross groove structure with the same lattice parameters.

(a)　　　　　　　　　　　　　　　　　　　(b)
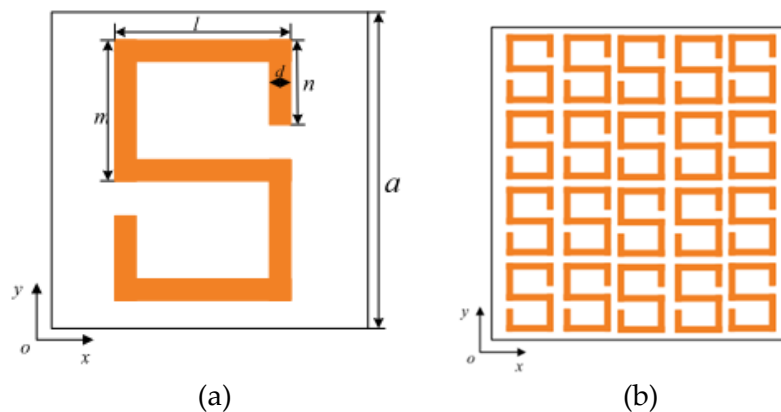
Figure 14. Schematic diagram of proposed structures: (**a**) The unit cell of an S-shape slot phononic crystal (PC); (**b**) Schematic view of the cross-section of the two-dimensional PC [54].

In 2017, Xia et al. [55] designed a spatially coiled acoustic metamaterial based on the Hilbert fractal structure (see Figure 15). It is found through research that the high-order Hilbert fractal structure can effectively realize sub-wavelength filtering, and as the fractal order increases, the number of band gaps of the metamaterial increases and the total band gap width gradually becomes larger.
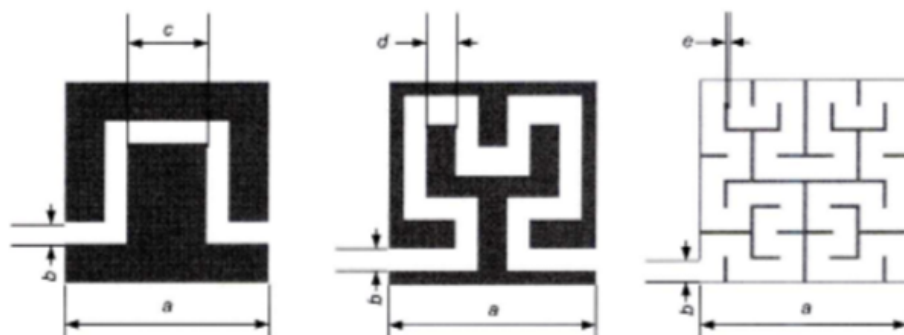

Figure 15. Space coiled acoustic metamaterials based on Hilbert fractals: first-order fractal, second-order fractal, and third-order fractal [55].

In 2019, Dong et al. [56] proposed a new structure with broadband double-negativity based on the cavity structure and spatial curling mechanism, revealing the most useful topological characteristics of metamaterials based on the above structures, and two typical The negative refraction and sub-wavelength imaging of the structure were detailed numerically simulated. The same year, Wu et al. [57] proposed a hybrid acoustic metamaterial composed of micro-perforated plates (MPP) and curled Fabry-Perot (FP) channels (see Figures 16 and 17), and found that the material works at a frequency greater than 30 times the total thickness. At the resonance frequency (<500 Hz), the sound absorption effect can reach

99%. The sound absorption performance of this material is mainly caused by the frictional loss of sound wave energy in MPP.

This resonance from the folded space produces a very wide band refractive index with a small absorption loss and a negative broadband response. Meanwhile, this kind of structure has a high requirement for manufacturing which may make them very expensive. Later, we can adopt a proper strategy to design acoustic metamaterials with new geometric structures.
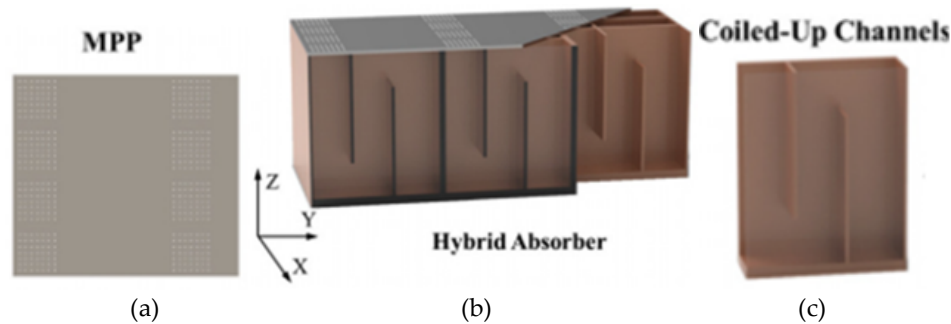
Figure 16. Schematic diagram of proposed structure: (**a**) The top micro-perforated panel; (**b**) Schematic of the hybrid metamaterial absorber; (**c**) Diagram of one coiled-up FP channel [57].
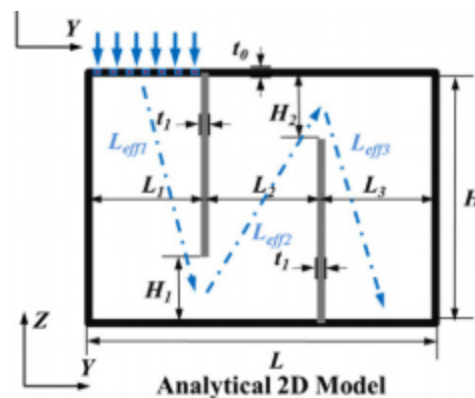
Figure 17. An approximate analytical two-dimensional (2D) model of a unit cell of a space-coiled metamaterial [57].

4.5. Other Structures

In addition to the above four structures, some other acoustic metamaterial structures have also been developed. Here we discuss some other types. Based on soft technology, a class of local resonance ultrasonic super-liquids composed of macroporous microsphere concentrated suspensions were designed. The negative index of metamaterials is derived from the low-frequency resonance of subwavelength particles. In 2015, Ouyang et al. [58] used elastic membranes to make hollow spheres. The interior of the sphere is filled with air to obtain a soft resonance unit. The resonance frequency is around 860 Hz, and the propagation loss of sound waves is 11 dB. A band gap is generated near the resonance frequency. Good sound insulation. The same year, Leroy et al. [59] studied bubble resonators, which are single-layer gas inclusions in soft solids. This bubble ultrafiltration membrane can be used as an ultra-thin coating to achieve acoustic super absorption over a wide frequency range.

In 2016, Wang et al. [60] proposed an acoustic metamaterial with periodic spindle-shaped inclusions embedded in a rubber matrix (see Figure 18). This structure can generate a large complete band gap in the range of 163–222 Hz, and the generation of the forbidden band is mainly due to the recirculation motion and shear motion of the matrix around the inclusions.

The acoustic black hole phenomenon is a promising method for controlling vibration, which has attracted more and more attention of scholars in recent years. The black hole phenomenon originates

from astrophysics and refers to a space-time region of sufficient mass that can absorb any material outside the region, and the absorbed material (including photons) cannot escape.

(a)　　　　　　　　　　　　　　　　　　　(b)
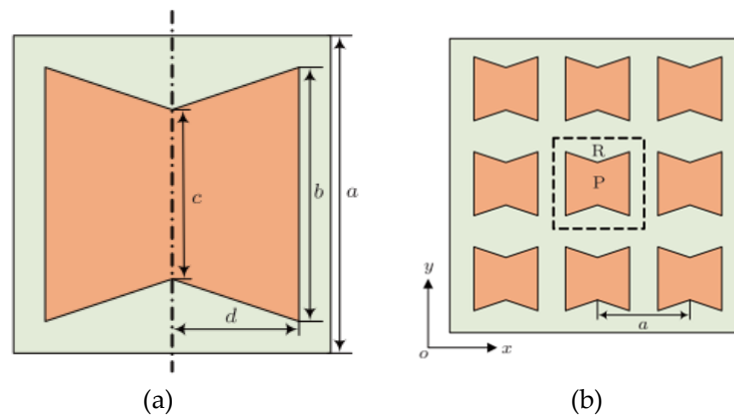
Figure 18. (**a**) The unit cell with spindle-shaped inclusion; (**b**) Schematic view of proposed PC [60].

In 1988, Mironov found a similar phenomenon in a wedge-shaped structure. When the thickness of the thin plate structure is reduced as a power function ($h(x) = Ax^m$, $m \geq 2$), the wave velocity of the bending wave will gradually decrease with the decrease of the thickness. Under ideal conditions, the wave velocity can be reduced. Wave reflections as small as zero are achieved [61,62]. In 2019, Liu et al. [63] designed an acoustic superstructure by embedding multiple acoustic black hole units in an array on a 10 mm thin plate (see Figure 19). It was found through experiments that the average sound insulation of the structure in the frequency band of 50–160 Hz can reach nearly 30 dB, and the average sound insulation in the frequency band of 100–600 Hz can reach 40 dB.
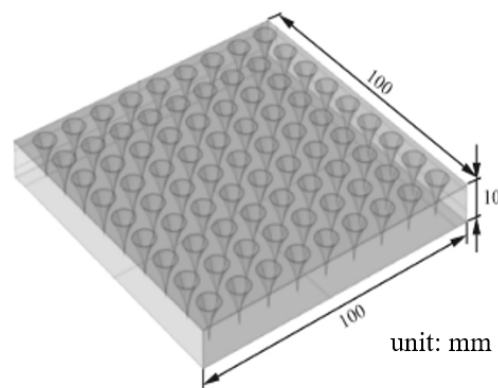
Figure 19. The diagram of the ideally designed acoustic black hole superstructure [63].

Only some common configurations are listed here, and there are many other acoustic metamaterial configurations, all of which can produce band gaps to suppress elastic propagation. However, acoustic metamaterials with lower frequency band and wider frequency range to meet engineering needs are still needed.

5. The Extraordinary Properties of Acoustic Metamaterials and Phononic Crystals

In physics, dielectric constant and permeability are two basic parameters that describe the properties of electromagnetic fields in a homogeneous medium. In recent years, scholars have designed many electromagnetic metamaterials with negative permittivity and negative permeability. These electromagnetic metamaterials have special properties such as negative refractive effect, perfect lens effect, anomalous Cherenkov radiation, and anomalous Doppler effects. Based on the similarity of electromagnetic waves and acoustic waves, acoustic metamaterials have become an emerging research hotspot. Acoustic metamaterials

with negative bulk modulus and negative mass density also exhibit unusual characteristics different from natural materials such as negative refraction, anomalous Doppler effect, amplified evanescent wave, and perfect sound absorption effect [16,64,65].

5.1. Negative Refraction Effect of Acoustic Waves [66]

Optical metamaterials have negative refractive indices related with the permittivity and permeability, while the acoustic metamaterials' negative refraction is determined by the effective mass density and bulk modulus. Sound waves have the nature of waves, and reflection and refraction occur at the interface between two media. And negative refraction occurs when acoustic waves scatter at the surfaces in the phononic crystals, leading to strong deformation [66]. Sound waves follow Snell's law when they are refracted, that is, they satisfy the following equations:

$$n_1 \sin \theta_1 = n_2 \sin \theta_2 \tag{1}$$

where n_1 and n_2 are the refractive indices of the two media, θ_1 and θ_2 are the angles of incidence and refraction, respectively. The material properties on both sides of the interface are different, and the nature of refraction is also different. When both sides are regular materials, both sides have a positive refractive index and positive refraction occurs; when one side is a normal medium and the other side is a special medium with a negative refractive index, negative refraction will occur (see Figure 20).
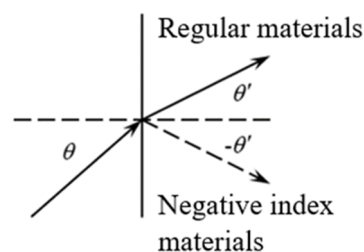

Figure 20. Negative refraction effect [63].

A lot of research has been done on the negative refraction effect of phononic crystals. Yang et al. [67] studied a phononic focusing phenomenon in the passband over a complete band gap in a 3D phononic crystal and found that the wave propagation depends largely on the frequency and the direction of incidence, and due to the anisotropy of the propagation, very large negative refraction occurs. In 2019, Mokhtari et al. [68] proposed the metamaterial properties of a two-phase unit cell traditionally considered to be a non-local resonance type, and demonstrated a hexagonal unit cell composed of two materials. They found that within the appropriate frequency range, the effective shear modulus and density are both negative and can produce negative refraction. That same year, Nemat-Nasser et al. [69] proved through experiments that the simple two-dimensional phononic crystals composed of aluminum matrix and circular flexible inclusions with square patterns have negative refractive characteristics in the shear mode and longitudinal mode. Dong et al. [56] proposed a space-curled metamaterial based on a broadband double-negative resonator and spatial winding mechanism, and verified the double-negative characteristics and negative refraction of the material through a large number of numerical simulations.

5.2. Anomalous Doppler Effect

The Doppler effect of natural materials is described as: the wave receiving frequency becomes higher when the wave source moves toward the observer, and the wave receiving frequency becomes lower when the wave source moves away from the observer. In a metamaterial with a negative refractive index, an anomalous Doppler effect occurs. When the wave source faces the observer, the frequency received by the observer decreases, and vice versa.

In 1968, Veselago [6] first theoretically predicted that metamaterials with negative refractive indices could produce anomalous Doppler phenomena. In 2010, Lee et al. [70] used one-dimensional long-period tubes to periodically arrange thin films and open holes on the side to prepare one-dimensional double-negative acoustic composites. The abnormal Doppler phenomenon was tested with a moving sound source. In 2015, Zhai et al. [71] designed an acoustic metamaterial with seven flute-like binary molecular clusters. Their research found that this metamaterial has both local elastic modulus and local density of mass density, and can achieve negative refraction over a wide frequency range, and also exhibit broadband reverse Doppler effect. In 2017, Liu et al. [72] further studied this structure and designed a test device to measure the Doppler effect. The experimental results show that in the negative refraction region of the acoustic metamaterial, when the sound source frequency is 2000 Hz: when the sound source is close, the ratio of the frequency detected by the detector to the sound source is reduced by 0.73 Hz; when the sound source is far away, the detector detects it compared to the increase of 0.68 Hz. In 2018, Zhai et al. [73] reported anomalous Doppler effects found in two commonly used wind instruments based on flute-type acoustic metamaterials. They found that both wind instruments can observe anomalous Doppler effects in the frequency range of two different speeds and ascending scales.

5.3. Enlargement of the Evanescent Wave

When sound waves propagate in both media, evanescent waves and propagating waves that carry sound wave information are generated. Because of the characteristic that evanescent waves disappear rapidly with increasing distance during propagation, the accuracy of acoustic imaging cannot be achieved at sub-wavelength size. In order to break through the sub-wavelength imaging problem, it is necessary to realize that the acoustic wave information of the evanescent wave is not lost. In the field of electromagnetics, based on the left-handed material with a refractive index of −1 proposed by Veselago [6], the flat lens effect can be achieved. Pendry [74] proposed that metamaterials can be designed by using metamaterials so that the evanescent wave is amplified by the superlens propagation. When the evanescent wave leaves the perfect lens, it begins to reduce rapidly to the original level, and theoretically a perfect image can be formed (see Figure 21).


(a)   (b)
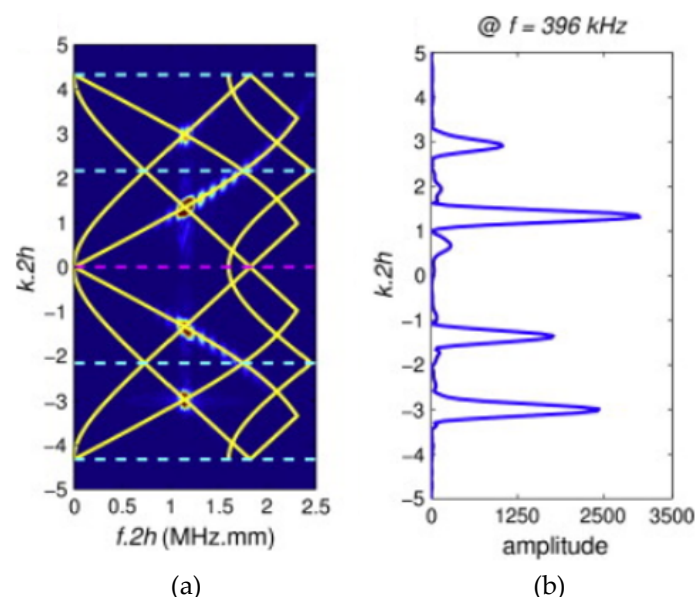
Figure 21. (**a**) Wavenumber-frequency representation of the signals measured under the grating for an excitation frequency belonging to the gap; (**b**) Amplitude versus wavenumber at a frequency f = 396 kHz [75].

According to the analogy of optical super-lens research, it can be found that the method to achieve acoustic sub-wavelength imaging is to enlarge the evanescent wave so that the evanescent wave

propagating in the near field can propagate to the far field imaging. In 2007, an acoustic metamaterial with negative equivalent mass density was proposed by Ambati et al. [76] that can amplify evanescent waves. Based on the above theory, in 2011, Park et al. [77] designed a metamaterial plate that can amplify evanescent waves. Park et al. believe that expanding the evanescent wave must reduce its loss, and requires that the imaginary part of its equivalent mass density is much smaller than the real part. They improved the negative mass density material composed of a fluid that can be embedded with a floating double resonator, and used a structure to cover the double resonator with a thin film to avoid losses. After the double resonator is covered with a thin film, the thin film blocks the liquid, allowing the liquid to move with the entire dual resonator, thereby reducing losses. This structure also has the advantage that the thin film can support the dual resonator and make it in a suitable position. Further research, taking out the dual resonator from this structure, still can obtain the material with negative mass density. At this time, the structure made of a stretched film can still amplify the evanescent wave. There are 16 thin film structures arranged in the x direction and eight arranged in the z direction to form a metamaterial system with negative mass density (see Figure 22d). After calculation, the imaginary part of the mass density is about 4% of the real part, the energy loss is very small, and the net amplitude gain of the evanescent wave emerging from the surface of the metamaterial system reaches 17 times.

In 2019, Zhang et al. [78] proposed an acoustic metamaterial composed of rubber cylinders arranged in a cubic lattice manner in an aqueous medium (see Figure 23). Using the finite-difference time-domain method (FDTD), they found that this interface mode can be used to enhance the transmission of evanescent waves and achieve subwavelength imaging.

(a)   (b)   (c)

(d)   (e)
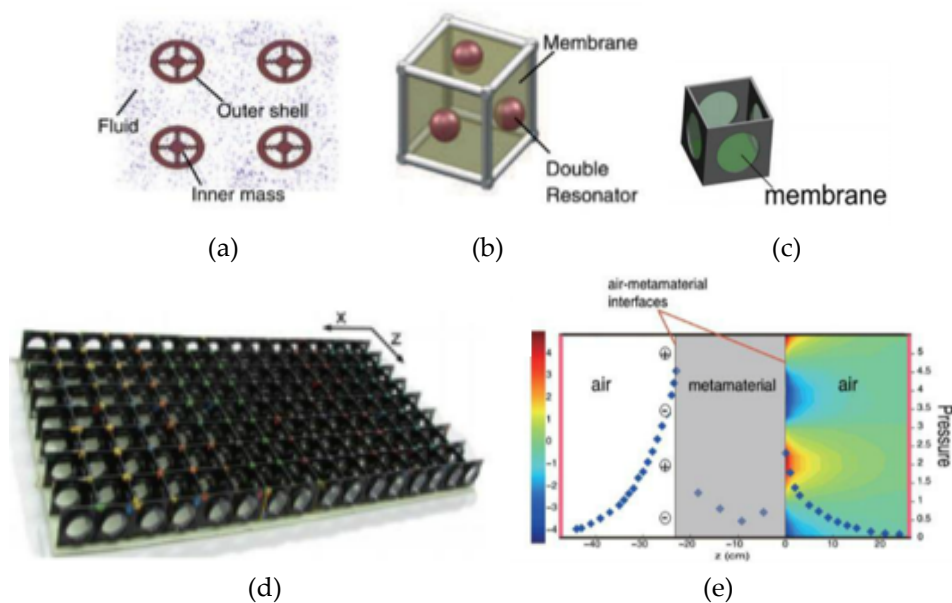
Figure 22. (**a**–**c**) Evolution of a floating double resonator to a thin film structure; (**d**) Negative mass density system; (**e**) Amplified evanescent wave [77].
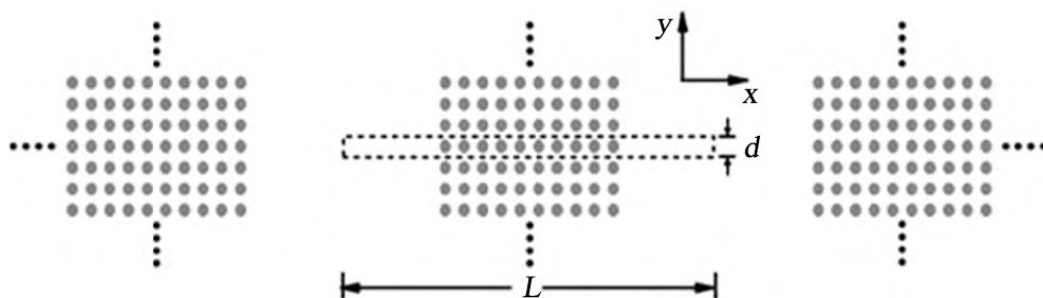

Figure 23. Supercell for calculations of interface modes [78].

5.4. Perfect Sound Absorption Effects

The near-perfect sound absorption effect exhibited by acoustic metamaterials has attracted the interest of a large number of researchers, and the use of its sound absorption characteristics to manufacture sound-absorbing materials has also become a research focus in recent years. In 2010, Pai [79] reported that humans absorbed electromagnetic waves more than electromagnetic metamaterials, and theoretically proposed a wide-band elastic wave absorber to make it possible to use acoustic metamaterials to absorb sound waves.

For the difficult problem of low frequency sound attenuation, Mei et al. [80] designed a structure with a thin semi-circular metal plate attached to the film (see Figure 24). The structure is geometrically open, similar to a cavity system. This structure achieves wide-band sound absorption in the low frequency range of 100–1000 Hz, and the sound absorption rate reaches 86% at a frequency of 172 Hz. When the structure is made into a double-layer film structure, the sound absorption rate can reach 99% at the lowest resonance frequency.
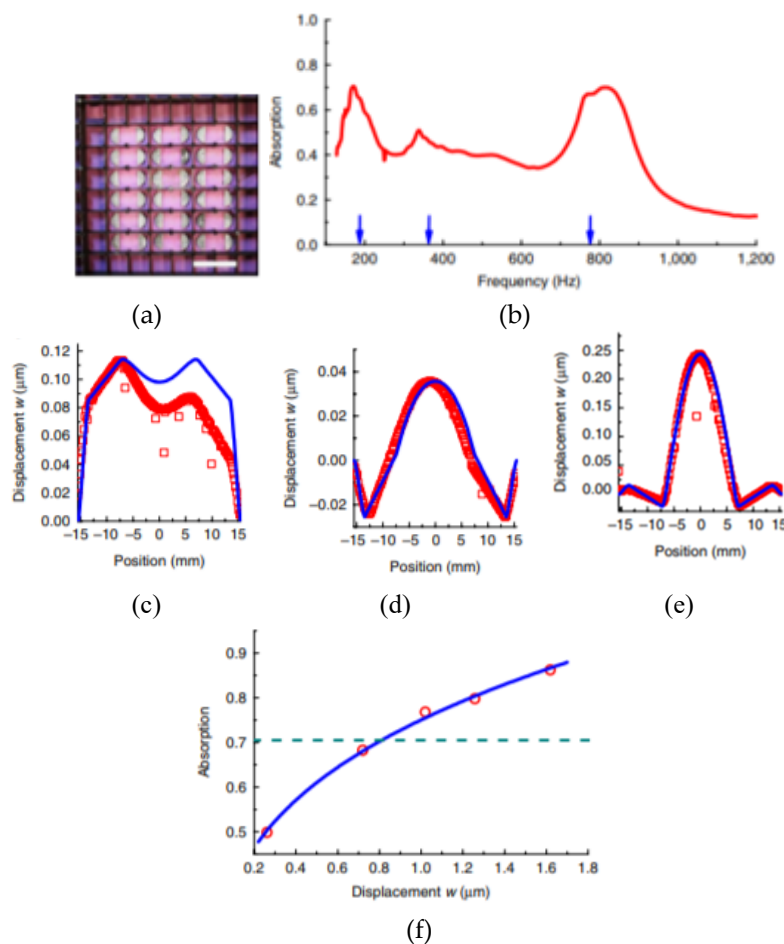
Figure 24. (**a**) Film structure diagram with a semi-circular metal sheet; (**b**) Broadband sound absorption diagram; (**c**–**e**) Sound absorption spectra at 172 Hz, 340 Hz, 813 Hz and displacement relationship of the film system; (**f**) Graph of sound absorption and displacement [80].

In 2018, Zhao et al. [81] designed an ultra-thin sub-wavelength absorber based on a regular coupling array that can achieve low-frequency absorption. They used a differential evolution algorithm to optimize the geometry of the coupled microslit, and improved the absorption of the microslit in the 300–800 Hz frequency band under different conditions. The ratio of the absorption thickness to the wavelength at the absorption peak was less than 3.4%, which proved that the absorption peak was in the deep Asia. The role of the wavelength region.

In 2019, Wu [82] proposed an acoustic metamaterial for low-frequency sound absorption consisting of three nested square-opened tubes and opposite opening directions (see Figure 25). The research found that the sound absorption at the sound absorption peak exceeds 90%, and the sound absorption frequency can be effectively adjusted by adjusting the geometric parameters of the sound absorber.

Figure 25. The diagram of the proposed structure [82].

In 2020, Ji et al. [83] compared the porous acoustic metamaterial with an inverted wedge shape on the plane interface with a uniform melamine layer and a classic wedge-shaped sound absorption material of the same quality. Better sound absorption at a range of frequencies and angles of incidence.

The above properties demonstrate the uniqueness of acoustic metamaterials. It's these extraordinary properties of acoustic metamaterials as well that lay a solid foundation for its special engineering application. These characteristics fill the gap in existing conventional material and point out the direction for further research. Some applications of acoustic metamaterials and phononic crystals are described below.

6. Application of Acoustic Metamaterials and Phononic Crystals

6.1. Acoustic Stealth Cloaks

In the field of electromagnetics, Leonhardt [84] and Pendry [85] et al. proposed in 2006 the use of conversion optics to achieve stealth. Using the method of conversion optics, the electromagnetic parameters of metamaterials are reasonably designed so that electromagnetic waves do not scatter when they pass through the hidden area, and guide the light around the object. After bypassing the metamaterial, the electromagnetic wave then travels along its original route. Due to the existence of the cloak, electromagnetic waves are transmitted or reflected on the cloak, and do not enter the area covered by the cloak. When an object is placed inside the cloak, the light will not spread inside the cloak, and the object will not be scattered, thereby achieving the effect of stealth. In summary, the working principle of the cloak is to construct a virtual space, that is, a wave-free space.

Based on the principle of conversion optics, Cummer et al. [86] determined the existence of a two-dimensional equation solution of transform acoustics with anisotropic mass in cylindrical coordinates, and theoretically discussed the possibility of acoustic stealth (see Figure 26). The acoustic transformation formula they proposed for the two-dimensional stealth cloak is as follows:

$$\rho_r = \frac{r}{r - R_1}, \rho_\phi = \frac{r - R_1}{r}, \lambda^{-1} = \left(\frac{R_2}{R_2 - R_1}\right)^2 \frac{r - R_1}{r} \tag{2}$$

where R_1 is the radius of the stealth area and R_2 is the outer radius of the stealth shell.

Based on the above two-dimensional theory, Chen et al. [87] used the expansion of the Bessel function series in spherical coordinates to solve the scattering problem. In 2008, Cummer et al. [88] verified the existence of a 3D acoustic wave stealth solution in fluids and the invariance of acoustic wave coordinate transformation, which established a theoretical basis for the proposed 3D stealth cloak. Cheng et al. [89] used homogeneous and isotropic materials to achieve two-dimensional acoustic

stealth of concentric alternating layered structure. Torrent et al. [90] used two-dimensional composite cylindrical structure to achieve two-dimensional acoustic stealth.


(a) (b)
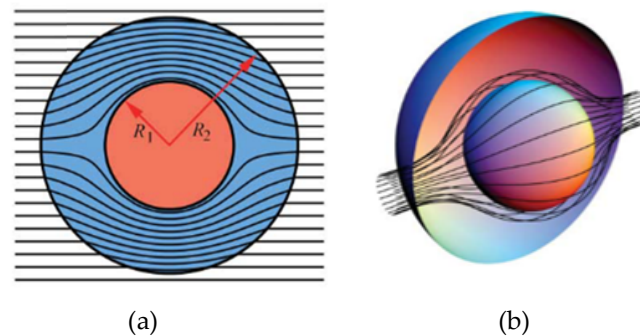
Figure 26. (**a**) Schematic diagram of a stealth cloak of 2D electromagnetic metamaterials; (**b**)Schematic diagram of a stealth cloak of 3D electromagnetic metamaterials [86].

The above are theoretically achieved acoustic stealth, in contrast, to achieve acoustic stealth in experiments is relatively hard. Stealth cloaks usually require the production of anisotropic materials. If one wants to achieve acoustic stealth in reality, one must find another way. In 2017, Chen et al. [91] proposed a ring-shaped underwater acoustic cape structure made of aluminum blocks (see Figure 27), achieving an average reduction of −6.3 dB in the frequency range of 9–15 kHz.


(a) (b)
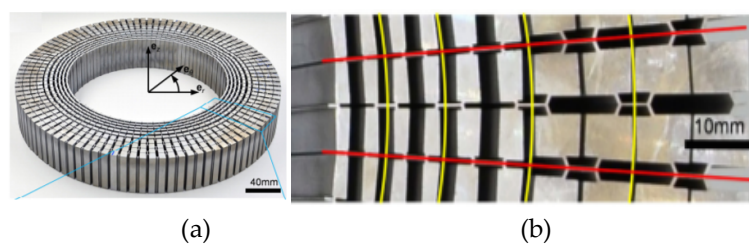
Figure 27. (**a**) Image of the cloak machined from an aluminum block; (**b**) Enlarged view of one segment, highlighted in (**a**) [91].

The same year, Bi et al. [92] designed an underwater carpet cape composed of multilayer brass plates by introducing a scale factor and sacrificing impedance matching (see Figure 28). Experimental results showed that the stealth carpet can hide the uneven information on the reflective surface in a wide frequency range.
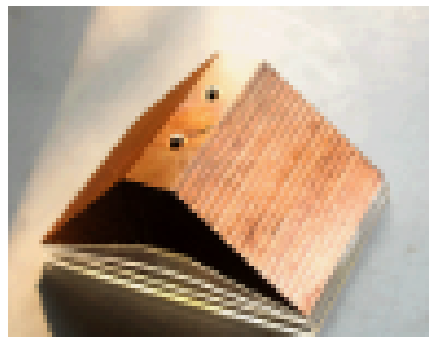
Figure 28. Experimental prototype of the carpet cloak [92].

In 2019, He et al. [93] proposed an ultra-thin planar stealth structure based on a periodic sound grid structure (see Figure 29). Through software simulation results, it was found that when the incident frequency was 300 kHz, the acoustic target intensity decreased (TSR) −5.425 dB.
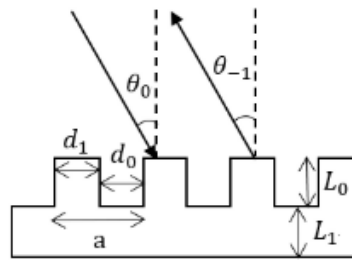
Figure 29. Acoustic metamaterial for ultrasound cloaking [93].

*6.2. Extraordinary Acoustic Abnormal Transmission Effects*

In 1998, Ebbesen et al. [94] realized the phenomenon of optical extraordinary transmission through a subwavelength hole array. Inspired by Ebbesen, Lu et al. [95] found that the sound wave's extraordinary transmission behavior through a one-dimensional grating achieves a sound transmittance close to 1. He et al. [96] sculpted periodical air grooves on both sides of a copper plate, and also achieved extraordinary sound transmission.

By changing the structural parameters, the curled space structure can also achieve the characteristics of metamaterials such as zero mass density, so the curled space structure can also achieve the extraordinary acoustic transmission effect. In 2015, Cheng et al. [97] designed a Mie resonance system with a curly space structure, as shown in Figure 30a. This Mie ultra-slow fluid-like unit has eight parts distributed uniformly, as shown in Figure 30b, and the simplified structure is shown in Figure 30c. In Figure 30d, a long and tortuous acoustic wave transmission channel is set, and the acoustic wave propagation path is compared after the acoustic metamaterial unit is placed. When not placed, the sound wave basically has no eye channel transmission. After being placed, most of the sound wave propagates through the channel. The results of the comparative experiments clearly show the ultrasonic transmission capability of the Mie resonance unit.


(a)　　　　　　　　　　　(b)　　　　　　　　　　　(c)

(d)
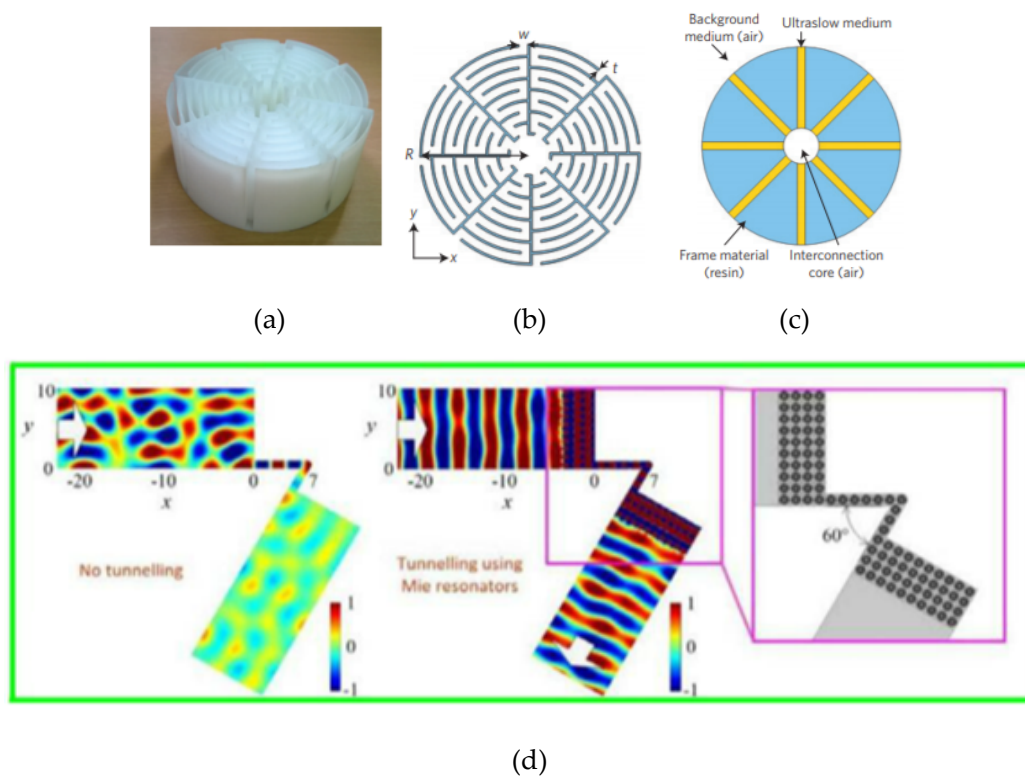
Figure 30. (**a–c**) Mie resonant unit with coiled space structure; (**d**) Meta-acoustic transmission of metamaterials [97].

In 2018, Dong et al. [98] proposed an acoustic super lens based on the idea of far-field acoustic super-resolution (see Figure 31). It was found that the far-field super-resolution of $\lambda/6$ can be achieved by using a multiple signal classification algorithm combined with a supersonic lens.
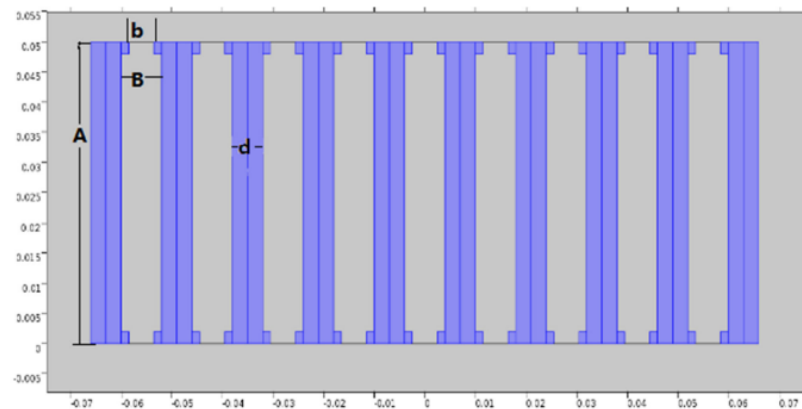
Figure 31. A schematic diagram of an acoustic superlens [98].

In 2020, Dong et al. [99] designed a class of multi-cavity 2D and 3D acoustic metamaterials (AMMs), and converted the 3D structure into a super lens (see Figure 32).


(a) (b)
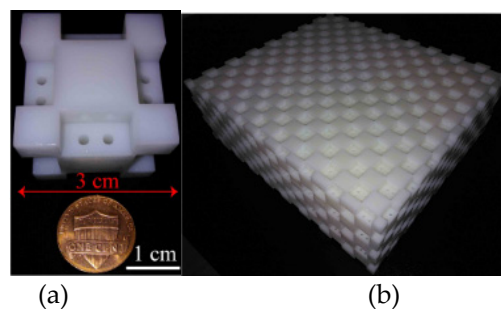
Figure 32. (**a**) Fabricated 3D microstructure sample; (**b**) Photograph of a 3D superlens containing 8 × 9 × 3 microstructures [99].

Numerical and experimental verifications show that the intensity distribution measured by the 3D superlens indicates that the sub-wavelength resolution is $0.46\lambda_0$, and two well-focused points can be obtained regardless of the phase shift. Secondly, due to the highly symmetrical 3D AMM, acoustic imaging can be achieved with normal incidence on each face of the sample.

6.3. Underwater Sound Absorption

In 2019, Zhong et al. [100] put forward the two theoretical requirements for the ultra-thin acoustic surface to fully absorb low-frequency underwater acoustic broadband under the action of semi-infinite air, and based on this, designed a rubber periodically embedded in the cavity (see Figure 33). The layer is acoustically super-surface and achieves perfect sound absorption at a frequency of 500 Hz.

The same year, Shi et al. [101] designed a multilayer local resonance scattering body based on the local resonance mechanism and the idea of coupled resonance (see Figure 34). They used finite element analysis to study the band gap characteristics and sound absorption characteristics of the proposed multilayered locally resonant acoustic metamaterials (M-LRAMs). Numerical results show that M-LRAMs have more obvious advantages in underwater sound absorption than traditional locally resonant acoustic metamaterials (LRAMs).
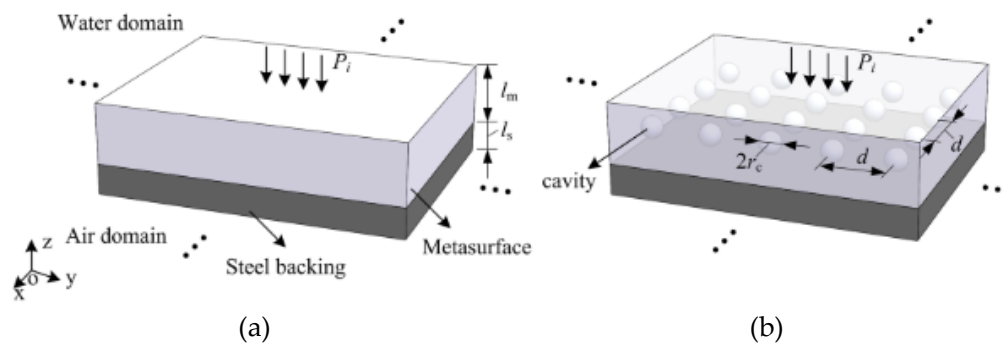
Figure 33. (**a**) A schematic view of an underwater absorptive metasurface with a finite-thickness steel plate followed by air; (**b**) A physical realization of the proposed metasurface for perfect absorption [100].
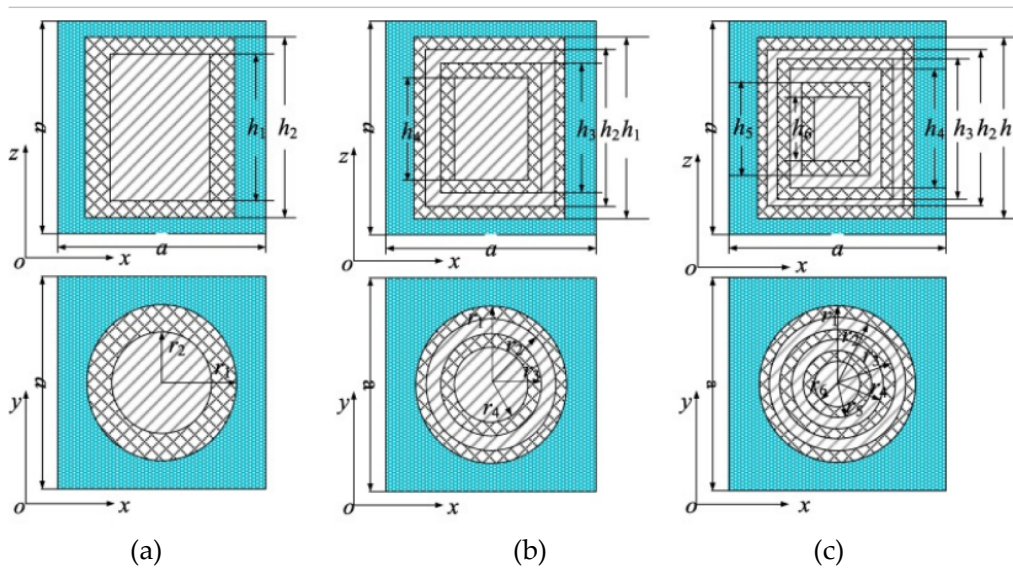
Figure 34. The cross-section for a unit cell of the three proposed devices: (**a**) Conventional LRAMs; (**b**) LRAMs with double-layered cylindrical scatterers; (**c**) LRAMs with three-layered cylindrical scatterers [101].

The same year, Zhong et al. [102] proposed a metamaterial sheet consisting of a particle-filled polyurethane damping material and a square lattice of a spiral resonator. Based on theoretical calculations and experimental results, they found that the average sound absorption coefficient of the proposed metamaterial board in the frequency range of 0.8–6 kHz is 0.54 at normal atmospheric pressure. Further research found that the average sound absorption coefficient of the metamaterial board can reach 0.51 under the conditions that the pressure is lower than 0.5 MPa and the frequency range is 1.5–6 kHz.

6.4. Other Applications

Over the past ten years, due to the strange properties of acoustic metamaterials, acoustic metamaterials have been applied to many other aspects. Christensen et al. [103] achieved the acoustic collimation of longer-wavelength sound waves through a two-dimensional array of subwavelength holes in a metal film. Analogous to optical rainbows, Cox et al. [104] implemented acoustic rainbows using many thin perforated plates separated by half a wavelength. Liang et al. [105,106] have theoretically proposed and experimentally designed a simple 1D superlattice and an acoustic diode composed of nonlinear materials, which can change the original frequency *f* to *2f* to achieve the frequency doubling function. With the rapid development of acoustic metamaterials, its unique properties are constantly being discovered and applied to many new fields, such as architectural acoustics and so on.

7. Concluding Remarks

The study of phononic crystals and acoustic metamaterials not only has important scientific research value, but also great practical value. The discovery of phononic crystals and acoustic metamaterials provides a new solution for vibration isolation and sound absorption. Therefore, the research work on phononic crystals and acoustic metamaterials has attracted widespread attention from the academic community. In the future, research on acoustic metamaterials and phononic crystals can focus on the following directions:

(1)　Deepen the effect of lattice parameters, structural configurations, and material properties of phononic crystals and acoustic metamaterials on the band gap characteristics;

(2)　Based on existing research on phononic crystal forbidden bands, designing more phononic crystals with different materials, shapes and decreasing the lattice sizes to meet actual needs;

(3)　Continue to advance the research on the local resonance mechanism for acoustic metamaterials and strive to achieve the control of elastic waves in low frequency bands and broader width for forbidden bands;

(4)　Increase the experimental research of phononic crystals and acoustic metamateirals, and expand theoretical research to practical applications.

The exploration of phononic crystals is only a few decades old, and there are still many valuable materials and uses to be studied. With the deepening of research on phononic crystals, many practical acoustic metamaterials will be extended to promote the development of sound insulation and noise reduction.

References

1. He, W.; Wang, Z.; Ling, H. Environmental noise pollution and inspection and control measures (In Chinese). *Guangdong Chem. Ind.* **2016**, *43*, 123.
2. Ibrahim, R.A. Recent advances in nonlinear passive vibration isolators. *J. Sound Vib.* **2008**, *314*, 371–452. [CrossRef]
3. Gripp, J.A.B.; Rade, D.A. Vibration and noise control using shunted piezoelectric transducers: A review. *Mech. Syst. Signal Pr.* **2018**, *112*, 359–383. [CrossRef]
4. Aditya, L.; Mahlia, T.M.I.; Rismanchi, B.; Ng, H.M.; Hasan, M.H.; Metselaar, H.S.C.; Muraza, O.; Aditiya, H.B. A review on insulation materials for energy conservation in buildings. *Renew. Sust. Eenrg. Rev.* **2017**, *73*, 1352–1365. [CrossRef]
5. Wu, J. Application of acoustic metamaterials in low-frequency vibration and noise reduction (In Chinese). *J. Mech. Eng.* **2016**, *52*, 68–78. [CrossRef]
6. Veselago, V.G. The electrodynamics of substances with simultaneously negative values of e and μ. *Sov. Phys. Usp.* **1968**, *10*, 509–514. [CrossRef]
7. Peng, H.; Pai, P. Acoustic metamaterial plates for elastic wave absorption and structural vibration suppression. *Int. J. Mech. Sci.* **2014**, *89*, 350–361. [CrossRef]
8. Wen, J.; Han, X.; Wang, G.; Zhao, H.; Liu, Y. Review of phononic crystals (In Chinese). *J. Func. Mater.* **2003**, *34*, 364–367.
9. Wu, Z.; Xu, S. Prospects for application of acoustic metamaterials and structure engineering (In Chinese). *Audio Eng.* **2017**, *41*, 16–27.
10. John, S. Strong localization of photons in certain disordered dielectric superlattices. *Phys. Rev. Lett.* **1987**, *58*, 2486–2489. [CrossRef]
11. Yablonovitch, E. Inhibited spontaneous emission in solid-state physics and electronics. *Phys. Rev. Lett.* **1987**, *58*, 2059–2062. [CrossRef] [PubMed]
12. Li, Y.; Chen, T.; Wang, X.; Ma, T.; Jiang, P. Acoustic confinement and waveguiding in two-dimensional phononic crystals with material defect states. *J. Appl. Phys.* **2014**, *116*, 024904. [CrossRef]

13. Sigalas, M.M.; Economou, E.N. Elastic and acoustic wave band structure. *J. Sound Vib.* **1992**, *158*, 377–382. [CrossRef]

14. Kushwaha, M.S.; Halevi, P.; Dobrzynski, L.; Djafari Rouhani, B. Acoustic band structure of periodic elastic composites. *Phys. Rev. Lett.* **1993**, *71*, 2022–2025. [CrossRef] [PubMed]

15. Wang, X.; Sun, H.; Chen, T.; Wang, X. Enhanced acoustic localization in the two-dimensional phononic crystals with slit tube defect. *Phys. Lett. A* **2019**, *383*, 125918. [CrossRef]

16. Lu, M.; Feng, L.; Chen, Y. Phononic crystals and acoustic metamaterials(In Chinese). *Mater. Today* **2009**, *12*, 25–32. [CrossRef]

17. Munjal, M.L. Response of a multi-layered infinite plate to an oblique plane wave by means of transfer matrices. *J. Sound Vib.* **1993**, *162*, 333–343. [CrossRef]

18. Sigalas, M.M.; Soukoulis, C.M. Elastic-wave propagation through disordered and/or absorptive layered systems. *Phys. Rev. B* **1995**, *51*, 2780–2789. [CrossRef]

19. Kushwaha, M.; Halevi, P.; Martínez, G.; Dobrzynski, L.; Djafari-Rouhani, B. Theory of acoustic band structure of periodic elastic composites. *Phys. Rev. B* **1994**, *49*, 2313–2322. [CrossRef]

20. Wu, F.; Liu, Z.; Liu, Y. Band structure of elastic waves in the two dimensional periodic composites (In Chinese). *Acta Acus.* **2001**, 319–323.

21. Qi, G.; Yang, S.; Bai, S.; Zhao, X. A study of the band structure in two-dimensional phononic crystals based on plane-wave algorithm (In Chinese). *Acta Phys. Sin.* **2003**, 154–157.

22. Wu, F.; Liu, Z.; Liu, Y. Acoustic band gaps in 2d liquid phononic crystals of rectangular structure. *J. Phys. D Appl. Phys.* **2001**, *35*, 162. [CrossRef]

23. Nikifor, R.; Arshad, M.; Mufei, X. Deposition-and-substrate tunable photonic bandgap in optical responses of hydrogenated amorphous silicon carbide thin films. *Mod. Phys. Lett. B* **2003**, *17*, 387–392.

24. Wu, F.; Hou, Z.; Liu, Z.; Liu, Y. Point defect states in two-dimensional phononic crystals. *Phys. Lett. A* **2001**, *292*, 198–202. [CrossRef]

25. Kushwaha, M.S. Stop-bands for periodic metallic rods: Sculptures that can filter the noise. *Appl. Phys. Lett.* **1997**, *70*, 3218. [CrossRef]

26. Zhao, H.; Han, X.; Wen, J.; Wang, G. Studies on phononic band gaps of periodic hollow cylinders in the air (In Chinese). *J. Mat. Sci. Eng.* **2004**, 71–73.

27. Sigalas, M.M. Defect states of acoustic waves in a two-dimensional lattice of solid cylinders. *J. Appl. Phys.* **1998**, *84*, 3026–3030. [CrossRef]

28. Kushwaha, M. Ultra-wide-band filter for noise control. *J. Acoust. Soc. Am.* **2008**, *124*, 2488. [CrossRef]

29. Wang, G.; Wen, J.; Han, X.; Zhao, H. Finite difference time domain method for the study of band gap in two-dimensional phononic crystals (In Chinese). *Acta Phys. Sin.* **2003**, *52*, 1943–1947.

30. Sigalas, M.M.; Garcia, N. Theoretical study of three dimensional elastic band gaps with the finite-difference time-domain method. *J. Appl. Phys.* **2000**, *87*, 3120–3122. [CrossRef]

31. Liu, Z.; Chan, C.T.; Sheng, P.; Goertzen, A.L.; Page, J.H. Elastic wave scattering by periodic structures of spherical objects: Theory and experiment. *Phys. Rev. B* **2000**, *62*, 2446–2457. [CrossRef]

32. Liu, Z.; Zhang, X.; Mao, Y.; Zhu, Y.Y.; Yang, Z.; Chan, C.T.; Sheng, P. Locally resonant sonic materials. *Science* **2000**, *289*, 1734–1736. [CrossRef] [PubMed]

33. Tian, Y.; Ge, H.; Lu, M.H.; Chen, Y.F. Research advances in acoustic metamaterials (In Chinese). *Acta Phys. Sin.* **2019**, *68*, 12.

34. Huang, H.H.; Sun, C.T. Theoretical investigation of the behavior of an acoustic metamaterial with extreme young's modulus. *J. Mech. Phys. Solids* **2011**, *59*, 2070–2081. [CrossRef]

35. Zhu, X.; Xiao, Y.; Wen, J.; Yu, D. Flexural wave band gaps and vibration reduction prop erties of a lo cally resonant stiffened plate (In Chinese). *Acta Phys. Sin.* **2016**, *65*, 316–330.

36. Wu, J.; Bai, X.C.; Xiao, Y.; Geng, X.M.; Yu, D.L.; Wen, J.H. Low frequency band gaps and vibration reduction prop erties of a multi-frequency lo cally resonant phononic plate (In Chinese). *Acta Phys. Sin.* **2016**, *65*, 209–219.

37. Ma, J.; Sheng, M.; Han, Y. Structure design and experimental verification of multi-bandgap locally resonant unit (In Chinese). *J. Vib. Eng.* **2019**, *32*, 943–949.

38. Fang, N.; Xi, D.; Xu, J.; Ambati, M.; Srituravanich, W.; Sun, C.; Zhang, X. Ultrasonic metamaterials with negative modulus. *Nat. Mater.* **2006**, *5*, 452–456. [CrossRef]

39. Jiang, J.; Yao, H.; Du, J.; Zhao, J.; Deng, T. Low frequency band gap characteristics of double-split helmholtz lo cally resonant periodic structures (In Chinese). *Acta Phys. Sin.* **2017**, *66*, 136–142.

40. Yu, D.; Shen, H.; Liu, J.; Yin, J.; Zhang, Z.; Wen, J. Propagation of acoustic waves in a fluid-filled pipe with periodic elastic helmholtz resonators (In Chinese). *Chin. Phys. B* **2018**, *27*, 064301. [CrossRef]

41. Smith, D.R.; Pendry, J.B.; Wiltshire, M.C.K. Metamaterials and negative refractive index. *Science* **2004**, *305*, 788–792. [CrossRef] [PubMed]

42. Pendry, J.B.; Holden, A.J.; Robbins, D.J.; Stewart, W.J. Magnetism from conductors and enhanced nonlinear phenomena. *IEEE T. Microw. Theory* **1999**, *47*, 2075–2084. [CrossRef]

43. Zhang, Z.; Zhu, H.; Luo, J.; Ma, B. The investigation on low-frequency broadband acoustic absorption performance of membrane sound-absorbing metamaterial (In Chinese). *J. Appl. Acoust.* **2019**, *38*, 869–875.

44. Hashimoto, N.; Katsura, M.; Yasuoka, M.; Fujii, H. Sound insulation of a rectangular thin membrane with additional weights. *Appl. Acoust.* **1991**, *33*, 21–43. [CrossRef]

45. Yang, Z.; Mei, J.; Min, Y.; Chan, N.; Ping, S. Membrane-type acoustic metamaterial with negative dynamic mass. *Phys. Rev. Lett.* **2008**, *101*, 204301. [CrossRef]

46. Yang, Z.; Dai, H.M.; Chan, N.H.; Ma, G.C.; Sheng, P. Acoustic metamaterial panels for sound attenuation in the 50–1000 hz regime. *Appl. Phys. Lett.* **2010**, *96*, 041906. [CrossRef]

47. He, Z.; Zhao, J.; Yao, H.; Jiang, J.; Chen, X. Sound insulation performance of thin-film acoustic metamaterials based on piezoelectric materials (In Chinese). *Acta Phys. Sin.* **2019**, *68*, 179–190.

48. Wang, T.; Sheng, M.; Guo, Z.; Qin, Q. Flexural wave suppression by an acoustic metamaterial plate. *Appl. Acoust.* **2016**, *114*, 118–124. [CrossRef]

49. Wang, T.; Sheng, M.; Ding, X.; Yan, X. Wave propagation and power flow in an acoustic metamaterial plate with lateral local resonance attachment. *J. Phys. D Appl. Phys.* **2018**, *51*. [CrossRef]

50. Zhou, G.; Wu, J.; Lu, K.; Tian, X.; Huang, W.; Zhu, K.D. Low-frequency sound insulation performance of membrane-type acoustic metamaterials with multi-state anti-resonance synergy(In Chinese). *J. Xi'an JiaoTong Univ.* **2020**, *54*, 64–74.

51. Li, Y.; Liang, B.; Zou, X.-Y.; Cheng, J.-C. Extraordinary acoustic transmission through ultrathin acoustic metamaterials by coiling up space. *Appl. Phys. Lett.* **2013**, *103*, 1–4.

52. Yong, L.; Liang, B.; Xu, T.; Zhu, X.F.; Zou, X.Y.; Cheng, J.C. Acoustic focusing by coiling up space. *Appl. Phys. Lett.* **2012**, *101*, 233508.

53. Li, Y.; Chen, T.; Wang, X.; Yu, K.; Song, R. Band structures in two-dimensional phononic crystals with periodic jerusalem cross slot. *Physica B* **2014**, *456*, 261–266. [CrossRef]

54. Wang, T.; Sheng, M.; Wang, H.; Qin, Q. Band structures in two-dimensional phononic crystals with periodic s-shaped slot. *Acoust. Aust.* **2015**, *43*, 1–6. [CrossRef]

55. Xia, B.; Liu, T.; Zheng, S.; Yu, D. Coiling up space acoustic metamaterial with hilbert fractal in a subwavelength scale (In Chinese). *Sci. Sin. Tech.* **2017**, *6*, 79–85.

56. Dong, H.; Zhao, S.; Wei, P.; Cheng, L.; Wang, Y.; Zhang, C. Systematic design and realization of double-negative acoustic metamaterials by topology optimization. *Acta Mater.* **2019**, *172*, 102–120. [CrossRef]

57. Wu, F.; Xiao, Y.; Yu, D.; Zhao, H.; Wang, Y.; Wen, J. Low-frequency sound absorption of hybrid absorber based on micro-perforated panel and coiled-up channels. *Appl. Phys. Lett.* **2019**, *114*, 151901. [CrossRef]

58. Ouyang, S.; Meng, Y.; JING, X. Investigation of a balloon-like soft resonator for negative-bulk-modulus acoustic metamaterials (In Chinese). *J. Nanjing Univ.* **2015**, *51*, 10–15.

59. Leroy, V.; Strybulevych, A.; Lanoy, M.; Lemoult, F.; Tourin, A.; Page, J.H. Superabsorption of acoustic waves with bubble metascreens. *Phys. Rev. B* **2015**, *91*, 020301. [CrossRef]

60. Wang, T.; Wang, H.; Sheng, M.; Qin, Q. Complete low-frequency bandgap in a two-dimensional phononic crystal with spindle-shaped inclusions. *Chin. Phys. B* **2016**, *25*, 288–295. [CrossRef]

61. Fang, H.; Zhou, K.; Song, Y. Introduction to acoustic black hole (In Chinese). *Coll. Phys.* **2013**, *32*, 30–41.

62. Krylov, V.V. Acoustic black holes: Recent developments in the theory and applications. *IEEE Trans. Ultrason. Ferroelectr. Freq. Control.* **2014**, *61*, 1296–1306. [CrossRef] [PubMed]

63. Liu, B.; Zhang, H.; Wang, K.; Wu, J. Acoustic black hole lightweight superstructure with low frequency broadband high efficiency sound insulation mechanism and experimental study (In Chinese). *J. Xi'an JiaoTong Univ.* **2019**, *53*, 128–134.

64. Ding, C.; Dong, Y.; Zhao, X. Research advances in acoustic metamaterials and metasurface (In Chinese). *Acta Phys. Sin.* **2018**, *67*, 10–23.

65. Ni, X.; Zhang, X.; Lu, M.; Chen, Y. Phononic crystals and acoustic metamaterials (In Chinese). *Physics* **2009**, *41*, 655–662.

66. Ge, H.; Yang, M.; Ma, C.; Lu, M.; Chen, Y.; Fang, N.; Sheng, P. Breaking the barriers: Advances in acoustic functional materials. *Natl. Sci. Rev.* **2018**, *5*, 159–182. [CrossRef]

67. Yang, S.; Page, J.H.; Liu, Z.; Cowan, M.L.; Chan, C.T.; Sheng, P. Focusing of sound in a 3d phononic crystal. *Phys. Rev. Lett.* **2004**, *93*, 024301. [CrossRef]

68. Mokhtari, A.A.; Lu, Y.; Srivastava, A. On the emergence of negative effective density and modulus in 2-phase phononic crystals. *J. Mech. Phys. Solids* **2019**, *126*, 256–271. [CrossRef]

69. Nemat Nasser, S. Inherent negative refraction on acoustic branch of two dimensional phononic crystals. *Mech. Mater.* **2019**, *132*, 1–8. [CrossRef]

70. Lee, S.H.; Park, C.M.; Yong, M.S.; Kim, C.K. Reversed doppler effect in double negative metamaterials. *Phys. Rev. B* **2010**, *81*, 145–173. [CrossRef]

71. Zhai, S.L.; Zhao, X.P.; Liu, S.; Shen, F.L.; Li, L.L.; Luo, C.R. Inverse doppler effects in broadband acoustic metamaterials. *Sci. Rep.* **2016**, *6*, 32388. [CrossRef]

72. Liu, S.; Luo, C.; Zhai, S.; Chen, H.; Zhao, X. Inverse doppler effect of acoustic metamaterial with negative mass density (In Chinese). *Acta Phys. Sin.* **2017**, *66*, 204–208.

73. Zhai, S.; Zhao, J.; Shen, F.; Li, L.; Zhao, X. Inverse doppler effects in pipe instruments. *Sci. Rep.* **2018**, *8*, 17833. [CrossRef] [PubMed]

74. Pendry, J.B. Negative refraction makes a perfect lens. *Phys. Rev. Lett.* **2000**, *85*, 3966–3969. [CrossRef] [PubMed]

75. Bavencoffe, M.; Morvan, B.; Hladky Hennion, A.C.; Izbicki, J.-L. Experimental and numerical study of evanescent waves in the mini stopband of a 1d phononic crystal. *Ultrasonics* **2013**, *53*, 313–319. [CrossRef] [PubMed]

76. Ambati, M.; Fang, N.; Sun, C.; Zhang, X. Surface resonant states and superlensing in acoustic metamaterials. *Phys. Rev. B* **2007**, *75*, 195447. [CrossRef]

77. Park, C.M.; Park, J.J.; Lee, S.H.; Yong, M.S.; Kim, C.K.; Lee, S.H. Amplification of acoustic evanescent waves using metamaterial slabs. *Phys. Rev. Lett.* **2011**, *107*, 194301. [CrossRef]

78. Zhang, F.; Liu, F. Acoustic interface waves in double-negative metamaterials (In Chinese). *J. Syn. Crystals* **2019**, *48*, 365–368.

79. Pai, P.F. Metamaterial-based broadband elastic wave absorber. *J. Intel. Mat. Syst. Str.* **2010**, *21*, 517–528. [CrossRef]

80. Mei, J.; Ma, G.; Yang, M.; Yang, Z.; Wen, W.; Sheng, P. Dark acoustic metamaterials as super absorbers for low-frequency sound. *Nat. Commun.* **2012**, *3*, 756. [CrossRef]

81. Zhao, H.; Wang, Y.; Wen, J.; Lam, Y.W.; Umnova, O. A slim subwavelength absorber based on coupled microslits. *Appl. Acoust.* **2018**, *142*, 11–17. [CrossRef]

82. Wu, P.; Mu, Q.; Wu, X.; Wang, L.; Li, X.; Zhou, Y.; Wang, S.; Huang, Y.; Wen, W. Acoustic absorbers at low frequency based on split-tube metamaterials. *Phys. Lett. A* **2019**, *383*, 2361–2366. [CrossRef]

83. Ji, G.; Fang, Y.; Zhou, J. Porous acoustic metamaterials in an inverted wedge shape. *Extreme Mech. Lett.* **2020**, *36*, 100648. [CrossRef]

84. Leonhardt, U. Optical conformal mapping. *Science* **2006**, *312*, 1777–1780. [CrossRef] [PubMed]

85. Pendry, J.B.; Schurig, D.; Smith, D.R. Controlling electromagnetic fields. *Science* **2006**, *312*, 1780–1782. [CrossRef]

86. Cummer, S.A.; Schurig, D. One path to acoustic cloaking. *New J. Phys.* **2007**, *9*, 45. [CrossRef]

87. Chen, H.; Chan, C.T. Acoustic cloaking in three dimensions using acoustic metamaterials. *Appl. Phys. Lett.* **2007**, *91*, 183518. [CrossRef]

88. Cummer, S.A.; Popa, B.I.; Schurig, D.; Smith, D.R.; Pendry, J.; Rahm, M.; Starr, A. Scattering theory derivation of a 3d acoustic cloaking shell. *Phys. Rev. Lett.* **2008**, *100*, 024301. [CrossRef]

89. Cheng, Y.; Yang, F.; Xu, J.Y.; Liu, X.J. A multilayer structured acoustic cloak with homogeneous isotropic materials. *Appl. Phys. Lett.* **2008**, *92*, 151913. [CrossRef]

90. Torrent, D.; Sánchez Dehesa, J. Acoustic cloaking in two dimensions: A feasible approach. *New J. Phys.* **2008**, *10*, 063015. [CrossRef]

91. Chen, Y.; Zheng, M.; Liu, X.; Bi, Y.; Sun, Z.; Xiang, P.; Yang, J.; Hu, G. Broadband solid cloak for underwater acoustics. *Phys. Rev. B* **2017**, *95*, 180104. [CrossRef]

92. Bi, Y.; Jia, H.; Lu, W.; Ji, P.; Yang, J. Design and demonstration of an underwater acoustic carpet cloak. *Sci. Rep.* **2017**, *7*, 705. [CrossRef] [PubMed]

93. He, J.; Jiang, X.; Ta, D. The ultrasound cloaking based on acoustic metamaterials (In Chinese). In Proceedings of the National Acoustic Conference in 2019, Shenzhen, China, 1–2 July 2019; Technical Acoustics: Shenzhen, China, 2019; p. 2.

94. Ebbesen, T.W.; Lezec, H.; Ghaemi, H.F.; Thio, T.; Wolff, P.A. Extraordinary optical transmission through sub-wavelength hole arrays. *Nature* **1998**, *391*, 667–669. [CrossRef]

95. Lu, M.; Liu, X.; Feng, L.; Li, J.; Huang, C.; Chen, Y.; Zhu, Y.; Zhu, S.; Ming, N. Extraordinary acoustic transmission through a 1d grating with very narrow apertures. *Phys. Rev. Lett.* **2007**, *99*, 174301. [CrossRef]

96. He, Z.; Jia, H.; Qiu, C.; Peng, S.; Mei, X.; Cai, F.; Peng, P.; Ke, M.; Liu, Z. Acoustic transmission enhancement through a periodically structured stiff plate without any opening. *Phys. Rev. Lett.* **2010**, *105*, 074301. [CrossRef]

97. Cheng, Y.; Zhou, C.; Yuan, B.G.; Wu, D.J.; Wei, Q.; Liu, X.J. Ultra-sparse metasurface for high reflection of low-frequency sound based on artificial mie resonances. *Nat. Mater.* **2015**, *14*, 1013–1019. [CrossRef]

98. Dong, Y.; Wang, P.; Yu, G. Far field super-resolution imaging based on an acoustic superlens (In Chinese). In Proceedings of the 2018 Acoustic Technology Academic Exchange Meeting of Four Provinces of Shandong, Zhejiang, Jiangsu and Heilongjiang, Qingdao, China, 20–22 September 2018; Technical Acoustics: Qingdao, China, 2018; p. 4.

99. Dong, H.; Zhao, S.; Wang, Y.; Cheng, L.; Zhang, C. Robust 2d/3d multi-polar acoustic metamaterials with broadband double negativity. *J. Mech. Phys. Solids* **2020**, *137*, 103889. [CrossRef]

100. Zhong, J.; Zhao, H.; Yang, H.; Wang, Y.; Yin, J.; Wen, J. Theoretical requirements and inverse design for broadband perfect absorption of low-frequency waterborne sound by ultrathin metasurface. *Sci. Rep.* **2019**, *9*, 1181. [CrossRef]

101. Shi, K.; Jin, G.; Liu, R.; Ye, T.; Xue, Y. Underwater sound absorption performance of acoustic metamaterials with multilayered locally resonant scatterers. *Results Phys.* **2019**, *12*, 132–142. [CrossRef]

102. Zhong, H.; Gu, Y.; Bao, B.; Wang, Q.; Wu, J. 2d underwater acoustic metamaterials incorporating a combination of particle-filled polyurethane and spiral-based local resonance mechanisms. *Compos. Struct.* **2019**, *220*, 1–10. [CrossRef]

103. Christensen, J.; Fernandez-Dominguez, A.I.; de Leon-Perez, F.; Martin-Moreno, L.; Garcia-Vidal, F.J. Collimation of sound assisted by acoustic surface waves. *Nat. Phys.* **2007**, *3*, 851–852. [CrossRef]

104. Cox, T.J. Acoustic iridescence. *J. Acoust. Soc. Am.* **2011**, *129*, 1165–1172. [CrossRef] [PubMed]

105. Liang, B.; Yuan, B.; Cheng, J. Acoustic diode: Rectification of acoustic energy flux in one-dimensional systems. *Phys. Rev. Lett.* **2009**, *103*, 104301. [CrossRef] [PubMed]

106. Liang, B.; Guo, X.S.; Tu, J.; Zhang, D.; Cheng, J.C. An acoustic rectifier. *Nat. Mater.* **2010**, *9*, 989–992. [CrossRef] [PubMed]